Building and Environment 45 (2010) 2273–2279

Contents lists available at ScienceDirect

Building and Environment

journal homepage: www.elsevier.com/locate/buildenv

The loss factors of building openings for wind-driven ventilation

Chia-Ren Chu*, Yu-Wen Wang

Department of Civil Engineering, National Central University, 300 Jhong-Da Road, Jhong-Li, Taoyuan, Taiwan 32001, R.O.C

ARTICLE INFO

Article history:
Received 28 January 2010
Received in revised form
16 April 2010
Accepted 16 April 2010

Keywords:
Wind-driven ventilation
Loss factor
Wind tunnel experiment
Partition
Resistance

ABSTRACT

This study used wind tunnel experiments to determine the loss factors of building openings for wind-driven ventilation. It is found that the loss factor is a function of internal porosity, but independent of Reynolds number. The loss factor of a partially open door increased as the door angle decreased. In addition, the influence of thickness ratio on the loss factor is much smaller than the internal porosity. The present study also derived the relationship between the loss factor and the discharge coefficient used in the orifice equation. The experimental results demonstrate that the ventilation rate of wind-driven cross ventilation can be predicted by a resistance model, once the loss factors of the openings and external pressure coefficients are known. Besides, it was found that the flow resistance of the internal opening dominated the ventilation rate when the external openings are large. But the resistance of external opening is the governing parameter when the external openings are small.

1. Introduction

Wind-driven natural ventilation is an effective way to maintain a comfortable and healthy indoor environment, especially for single-floor residential buildings [1–3]. A reliable prediction method is essential for the design and utilization of wind-driven ventilation. The most widely used method to calculate the volumetric flow rate, Q, through a building opening is the orifice equation [4,5]:

$$Q = C_d A \sqrt{\frac{2\Delta P}{\rho}} \quad (1)$$

where A is the cross-section area of the opening, ΔP is the pressure difference across the opening, ρ is the air density, and C_d is the discharge coefficient. This equation is derived from Bernoulli's assumption of irrotational, incompressible flow. Typical discharge coefficients given in the literature are in the range of 0.60–0.65 for sharp-edged openings [6–8]. It should be noticed that the pressure difference in Eq. (1) used in the ventilation studies is different from the pressure difference used for the orifice meter in pipe flows. In pipe flows, the pressure difference $\Delta P = P_1 - P_c$ is the difference between the pressure P_1 before the contraction and the pressure P_c at the contraction (or immediately after the contraction) [9]. However, in ventilation studies, because the room pressure is easier to measure than the pressure at the opening (contraction), $\Delta P = P_{r1} - P_{r2}$ is the difference of static pressure of two rooms [10,11]. The disparity in P_c and P_{r2} could cause inaccuracy when using orifice equation and typical discharge coefficient to calculate flow rate, especially when opening area is very small.

In addition, several studies [12–14] have pointed out that the use of the constant discharge coefficient constitutes an invalid simplification. Heiselberg and Sandberg [15] discussed the applicability of orifice equation to the external opening of buildings and pointed out that the discharge coefficient is difficult to determine and cannot be regarded as a constant. Santamouris [16] indicated that the value of C_d is dependent on the opening size. Tan and Glicksman [17] integrated CFD simulation with multi-zone model and suggested the internal discharge coefficient $C_d = 0.95$ for small internal openings, and $C_d = 0.70$ for vents and windows. Chu et al. [18], based on wind tunnel experiments, found that the discharge coefficient of external opening is dependent on the wind direction and opening Reynolds number.

Besides the problematic discharge coefficient, the flow resistance produced by internal doors inside the building cannot be accounted for using the orifice equation. The internal resistance generated by doors and obstacles in the path of the airflow will trim down the velocity and flow rate of wind-driven ventilation. This effect was neglected by most ventilation models that use orifice equation or power law equation to calculate the ventilation rate between different rooms. Hence, Kurabuchi et al. [19] and Ohba et al. [20] developed a "local dynamic similarity model" to replace the orifice equation. Aynsley [21] proposed a "resistance approach" to compute the flow rates through building openings.

* Corresponding author. Tel.: +886 3 4227151x34138; fax: +886 3 4252960.
E-mail addresses: crchu@cc.ncu.edu.tw (C.-R. Chu), sty03@hotmail.com (Y.-W. Wang).

0360-1323/$ – see front matter © 2010 Elsevier Ltd. All rights reserved.
doi:10.1016/j.buildenv.2010.04.010

The ventilation rate through an internal opening inside buildings can be derived from the energy equation:

$$\frac{P_{r1}}{\rho g}+z_1+\frac{V_1^2}{2g}=\frac{P_{r2}}{\rho g}+z_2+\frac{V_2^2}{2g}+k\frac{V_i^2}{2g} \tag{2}$$

where g is the gravitational acceleration, z is the elevation; P_r is the static pressures in the room (see Fig. 1); V is the average velocity in the room; subscripts 1 and 2 represent the room 1 and room 2, respectively. The last term on the right hand side is the energy loss when air pass through the internal opening, with V_i is the velocity at the opening, and k is the loss factor of the opening. In single-floor buildings, the difference in elevation $\Delta z = z_1 - z_2$ is negligible. When the cross-section areas of room 1 and room 2 are the same, $A_1 = A_2$; or the cross-sectional area of the room is much larger than opening area, the velocity head $V^2/2g$ on both sides of Eq. (2) can be neglected. Therefore, the definition of the loss factor is:

$$k=\frac{P_{r1}-P_{r2}}{\rho V_i^2/2} \tag{3}$$

Thus, the ventilation rate through the opening equals to:

$$Q=V_iA_i=A_i\sqrt{\frac{2\Delta P_i}{\rho\cdot k}} \tag{4}$$

where $\Delta P_i = P_{r1} - P_{r2}$ is the pressure difference of two adjacent rooms, A_i is the cross-sectional area of the internal opening. The loss factor k is a dimensionless coefficient, depending on the configuration of internal opening. By comparing Eq. (4) with the orifice equation Eq. (1), one can find the relationship between the loss factor and discharge coefficient:

$$k=C_d^{-2} \tag{5}$$

Eq. (4) can be used to calculate ventilation rate in partitioned buildings. For example, a building is partitioned into two rooms as shown in Fig. 1. The windward wall, leeward wall and internal partition each have one opening, and three openings are in series. Based on the continuity equation, the ventilation rates:

$$Q_1=Q_i=Q_2 \tag{6}$$

The ventilation rate can be derived from Eqs. (4) and (6):

$$\frac{Q_1}{U}=\left[\frac{C_{p1}-C_{p2}}{\frac{k_1}{A_1^2}+\frac{k_i}{A_i^2}+\frac{k_2}{A_2^2}}\right]^{1/2} \tag{7}$$

where U is the external wind velocity, C_p is the dimensionless pressure coefficient. In order to simplify above equation, the opening resistance is defined as:

$$\zeta=\frac{k}{A^2} \tag{8}$$

The unit of the resistance is [m^{-4}]. Therefore, the average velocity at the internal opening is:

$$\frac{u_i}{U}=\frac{1}{A_i}\left[\frac{C_{p1}-C_{p2}}{\zeta_1+\zeta_i+\zeta_2}\right]^{1/2} \tag{9}$$

The pressure difference between the windward and leeward openings is the driving force to overcome the resistances of cross ventilation. The smaller is the resistance ζ (and the loss factor k), the bigger is the ventilation rate Q. Eq. (9) can be used for buildings without internal partition ($\zeta_i = 0$), and buildings with partition ($\zeta_i \neq 0$). The internal resistance ζ_i becomes negligible when the internal opening area A_i is large. Eq. (7) is similar to the model proposed by Aynsley [21]. However, his definition of resistance is different from Eq. (8), and he did not verify his model with experimental data. Therefore, validation of this resistance model is needed.

On the other hand, Axley and Chung [22] pointed out that the building openings, such as windows and doors, are not typically sharp-edged orifices. They used the formula suggested by Idelchik [23] to calculate the loss factor for fluid passes through a thick-walled internal opening:

$$k=0.5(1-r_i)+(1-r_i)^2+\tau(1-r_i)^{0.5}(1-r_i) \tag{10}$$

where the internal porosity $r_i = A_i/A_w$ is defined as the ratio of the internal opening area A_i to the partition wall area A_w, and τ is the thickness correction parameter that can be determined using the following equation:

$$\tau=\left(2.4-t^*\right)\times 10^{-\left(0.25+\frac{0.535t^{*8}}{0.05+t^{*7}}\right)} \tag{11}$$

The thickness ratio $t^* = t/d$ is defined as the ratio of wall thickness t and opening size d. The typical value of thickness ratio for building openings is in the range of 5–50%, the claim of Axley and Chung [22] needed to be validated.

In this study, a series of wind tunnel experiments were carried out to investigate the influences of opening size, thickness ratio, Reynolds number and door angle on the loss factor. The experimental results were also used to verify Eqs. (9) and (10). Once the resistance model is verified, the building ventilation rate could be predicted when the loss factor k, external pressure coefficients C_{p1} and C_{p2}, opening areas are known.

2. Experimental setup

The experiments were carried out in an open-circuit, blowing-type wind tunnel. The total length of the wind tunnel is 8.3 m. The test section of wind tunnel is 1.2 m wide and 1.8 m long. A cubic model, with external dimensions of 0.40 m, was mounted on the centerline of the test section. The distance from the beginning of the test section to the model was 1.25 m. The schematic diagram of the experimental setup is shown in Fig. 2.

The surfaces of the model were made of smooth acrylic plate (thickness 4.8 mm) with square-shaped openings (size $d = 40$ mm, 60 mm and 100 mm) at the center of the plate. The space inside the model was equally separated into two zones by a partition plate. The internal lengths of rooms 1 and 2 both were 192.6 mm. The partition plate was also made of acrylic (width and height 390 mm, thickness 4.8 mm) with square-shaped openings (size $d_i = 20$ mm,

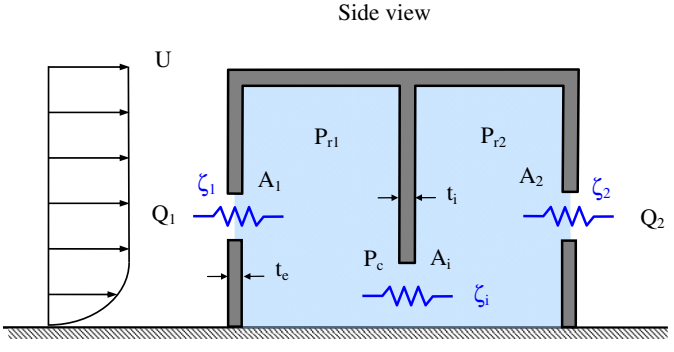

Fig. 1. Schematic diagram of opening resistance in a partitioned building.

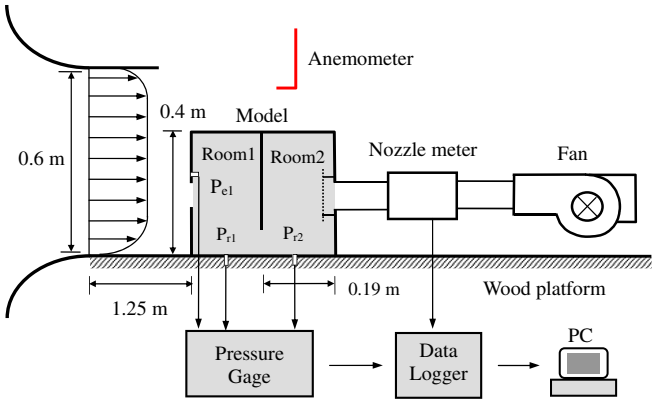

Fig. 2. Schematic diagram of experimental setup and building model.

30 mm, 40 mm, 50 mm, 60 mm, 80 mm and 100 mm) at the corner of the plate (see Fig. 3).

In order to investigate the effect of a partially open door on the airflow, an adjustable door (100 mm × 100 mm) was installed in the internal opening (100 mm × 100 mm). The door angle θ is adjustable, and is defined as the angle between the door and partition wall. Fig. 4 is the schematic diagram and photograph of the internal door.

The external pressures were measured by the pressure taps (diameter 1.5 mm, flush to the wall) 30 mm from the opening, and the pressure taps were connected to a multi-channel high-speed pressure transducer (ZOC33/64PX, Scanivalve Inc.) by short pneumatic tubings. The measuring range of the pressure sensor was ±2758 Pa, with a resolution of ±2.2 Pa. The sampling frequency was 100 Hz, and the sampling duration was 163.84 s.

At the beginning of the experiment, the internal pressures measured at different locations on the floor, ceiling and partition wall were compared, and it was found that the differences were within 1.26%. This indicated that the room pressure is fairly uniform, except the location that is very close to the opening. As a result, the pressure measured at the center of the floor of each room was used as the room pressure for the rest of the experiments. The external and internal pressures were measured as pressure differences from the reference static pressure near the inlet of the test section.

The fan technique described by Chiu and Etheridge [24] was adopted in this study to determine the loss factors of different opening configurations. The flow rate was controlled by a fan, and the mean flow rates were measured by nozzle meters. In this study,

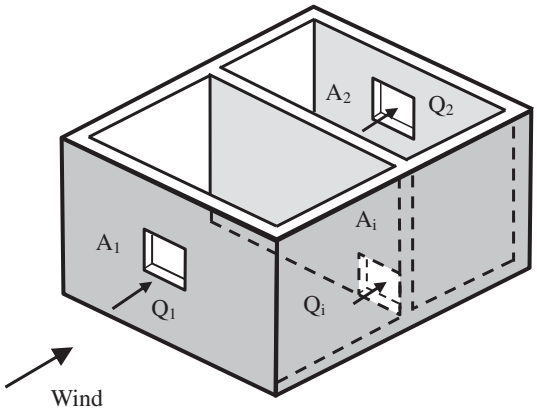

Fig. 3. Schematic diagram of the building model.

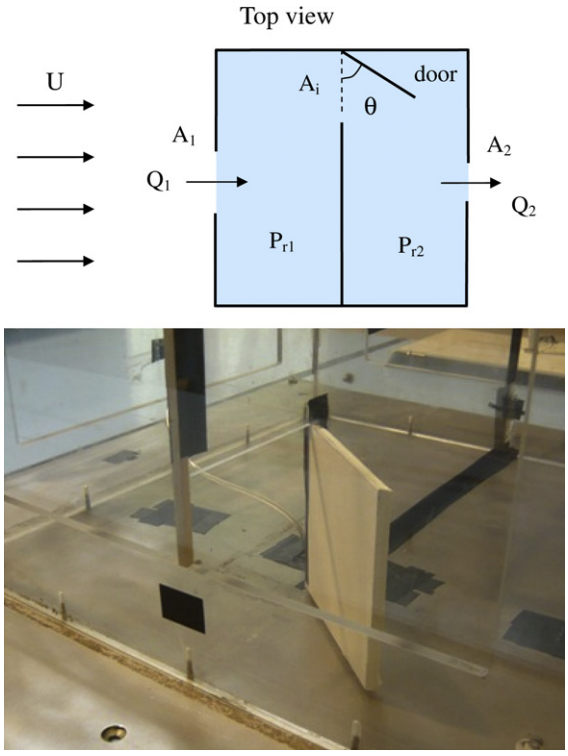

Fig. 4. Schematic diagram and photograph of partition wall and a partially open door.

five different sizes (diameters of the nozzle throat were 8 mm, 10 mm, 14 mm, 24 mm and 34 mm) of conical-shape nozzle meters were used for different flow rate ranges. The nozzle discharge coefficient was determined by [25]:

$$C_n = 0.9986 - \frac{7.006}{\sqrt{Re_n}} + \frac{134.6}{Re_n} \quad (12)$$

where the Reynolds number $Re_n = U_n d_n/\nu$, U_n is the velocity at the nozzle throat, d_n is the diameter of the nozzle throat, and ν is the kinematic viscosity of air.

A porous plate was installed at the leeward opening to alleviate the effects of suction on the flow field inside the model. The pressure differences across the building openings can then be measured. Chu et al. [26] used the same experimental setup and measured the velocities along the centerline of the windward opening inside the model, but without the internal partition. They found that the velocity distribution under natural wind-driven ventilation is close to that generated by the fan technique. In other words, this fan technique can correctly simulate the cross ventilation and accurately measure the ventilation rate and loss factor.

3. Results and discussion

3.1. Loss factors

This section discusses the experimental results of the loss factors of different opening configurations. The external wind speed $U = 17.5$ m/s, external wind direction (the incidence angle of the approaching flow to the windward façade) $\phi = 0°$. The leeward opening of the model was connected to a porous plate, a nozzle meter and a fan in this part of the experiment. The loss factor was calculated by Eq. (4), based on the measured flow rate Q and pressure difference ΔP_i.

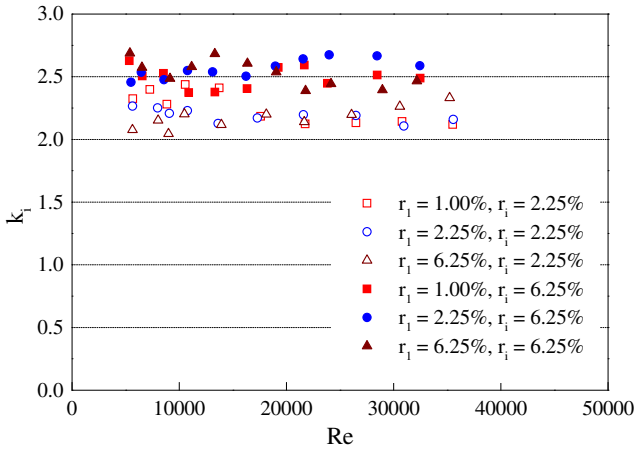

Fig. 5. Internal loss factor as a function of Reynolds number for external porosity r_1 = 1.0%, 2.25%, 6.25%, and internal porosity r_i = 2.25%, 6.25%.

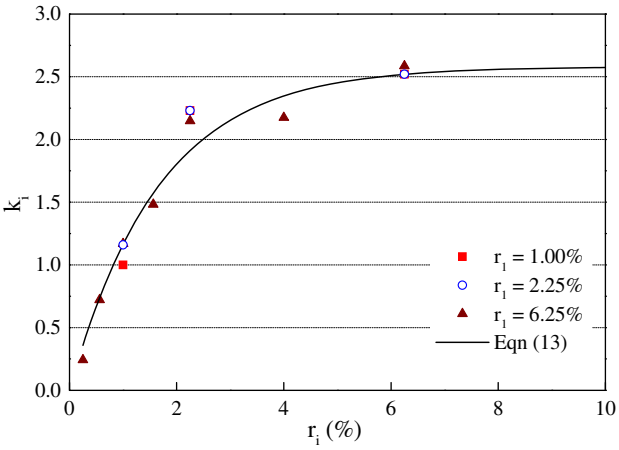

Fig. 7. Internal loss factor as a function of the internal porosity. The solid line is the prediction of Eq. (13).

Fig. 5 shows the relationship between the internal loss factor k_i and Reynolds number for internal porosity r_i = 2.25% and 6.25%. The opening Reynolds number is defined as:

$$\mathrm{Re} = \frac{u_i \times d_i}{\nu}$$

where $u_i = Q_i/A_i$ is the average velocity at the internal opening, d_i is the characteristic length of the internal opening, and ν is the kinematic viscosity of air. It is clear that the loss factors were independent of Reynolds number and the windward external porosity r_1 ($=A_1/A_w$). For internal porosity r_i = 6.25% (d_i = 100 mm), the average value of k_i = 2.53 and the corresponding discharge coefficient C_d = 0.629, as calculated by Eq. (5). This is in good agreement with the value C_d = 0.60–0.65 suggested by previous studies [6–8]. For r_i = 2.25% (d_i = 60 mm), the average value of k_i = 2.206. The resultant discharge coefficient C_d = 0.673 is slightly larger than that of r_i = 6.25%.

The loss factors of internal porosity r_i = 0.25–6.25% were shown in Fig. 6. External porosity r_1 = 6.25%, internal wall thickness t_i = 4.8 mm. The loss factor is independent of Reynolds number, just like the results shown in Fig. 5. But the loss factor decreased as the internal porosity (opening area) decreased. This is because the velocity V_i at the internal opening increased as the opening area A_i decreased. According to Eq. (3), the raise in the velocity head $V_i^2/2g$ produces a smaller loss factor.

Fig. 7 shows the loss factor as a function of internal porosity. By using regression analysis, an empirical equation between the loss factor k_i and internal porosity r_i can be found:

$$k_i = 2.58[1 - \exp(-60r_i)] \quad (13)$$

The coefficient of determination R^2 = 0.91. This equation indicates that the internal loss factor k_i = 2.58 for large opening (r_i > 5%). The corresponding discharge coefficient C_d = 0.622 agreed with the typical discharge coefficient C_d = 0.60–0.65 [6–8]. However, the discharge coefficient C_d increased as the opening area (and porosity r_i) decreased. For the internal porosity r_i = 1.0%, the loss factor k = 1.164. The corresponding discharge coefficient C_d = 0.927 is close the results of Tan and Glicksman [17], and Heiselberg et al. [13] for small internal openings.

The flow rates Q and pressure drops ΔP of different wall thickness (t_i = 4.8 mm, 10 mm, 15 mm, 20 mm and 40 mm) were measured to investigate the influence of wall thickness on the loss factor. Fig. 8 shows the relationship between the internal thickness ratio t_i^* ($= t_i/d_i$) and loss factor. The solid and dash lines are the predictions of Eq. (10) for internal porosity r_i = 1.0% and 6.25%, respectively.

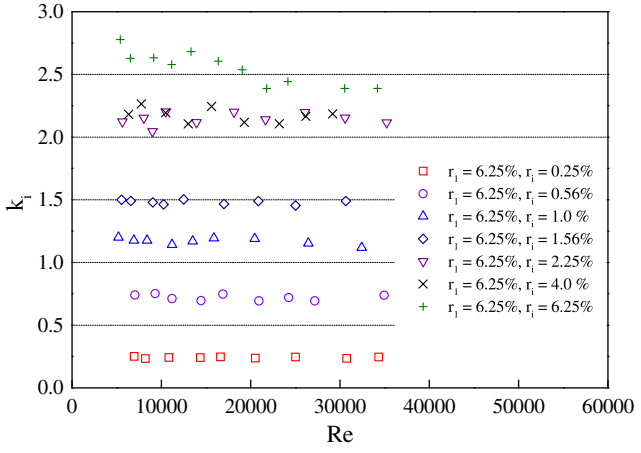

Fig. 6. Internal loss factor as a function of Reynolds number for internal porosity r_i = 0.25–6.25%. External porosity r_1 = 6.25%.

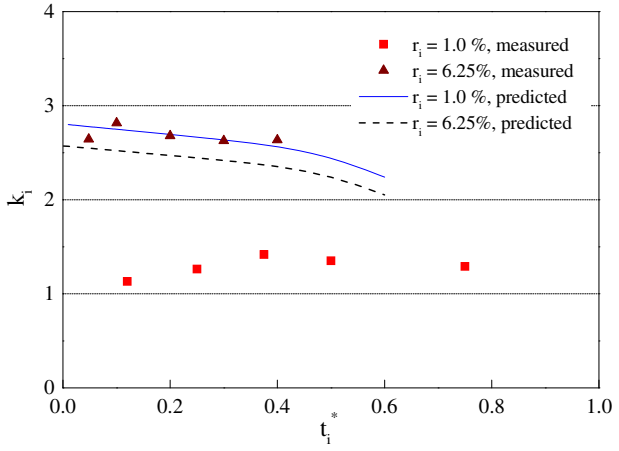

Fig. 8. Internal loss factor as a function of the internal thickness ratio t_i^* for internal porosity r_i = 1.0% and 6.25%. External porosity r_1 = 6.25% (d_i = 100 mm). The solid and dash lines are the predictions of Eq. (10).

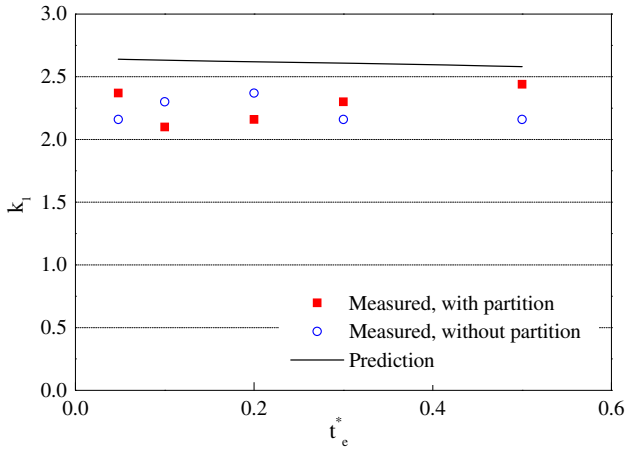

Fig. 9. External loss factor as a function of external thickness ratio t_e^*. External porosity $r_1 = 6.25\%$, internal porosity $r_i = 1.0\%$. The line is the predicted loss factor by the model of Idelchik [23].

As can be seen, the porosity is more influential than the thickness ratio on the loss factor (and discharge coefficient). The prediction of Eq. (10) is close to the measured loss factor k of $r_i = 6.25\%$, but is much larger than that of $r_i = 1.0\%$. In other words, Eq. (10) only can be used to predict the loss factors of large openings ($r_i > 5\%$). Based on the measured loss factors of $r_i = 6.25\%$, the variation of the loss factor for all five cases ($t_i^* = 4.8\%, 10\%, 20\%, 30\%, 40\%$) was within 6.7%. This implies that the influence of opening thickness on the internal loss factor (and discharge coefficient) can be neglected.

The relationship between the external loss factor k_1 and external thickness ratio $t_e^* (= t_e/d_e)$ was shown in Fig. 9. External porosity $r_1 = 6.25\%$, internal porosity $r_i = 1.0\%$. The line is the predicted loss factor for external opening by the model of Idelchik [23]. It can be seen that the measured loss factors are slightly smaller than the prediction, and external loss factors k_1 with internal partition (solid symbols) are close to the values without partition (empty symbols). This result revealed that the loss factor is independent of external thickness ratio and partition. The loss factors shown above are related to the internal opening without a door. The influence of a partially open door on the internal loss factor k_i is shown in Fig. 10. External porosity $r_1 = 6.25\%$, internal porosity $r_i = 6.25\%$, wall thickness $t_i = 4.8$ mm, and door angle $\theta = 30°, 60°, 90°$. The empty symbols represent the results without the adjustable door. The loss factors decreased as Reynolds number increased, and became

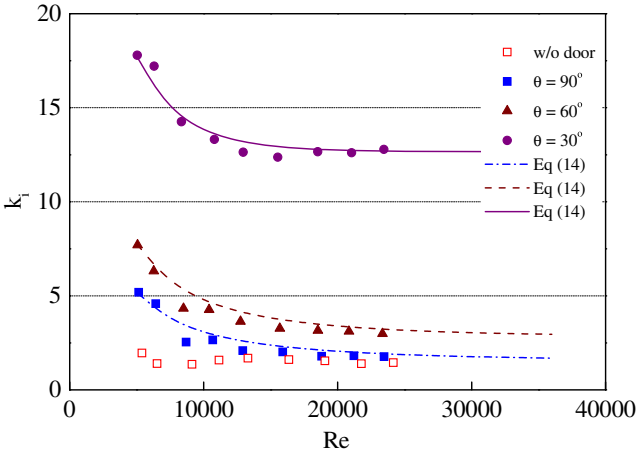

Fig. 10. Internal loss factor as a function of Reynolds number for different door angles. The empty symbols are the results without the adjustable door. The lines are the predictions of Eq. (14).

Table 1
Model coefficients for different door angles.

Door angle θ	k_o	Re_o	R^2
30°	12.658	4000	0.924
60°	2.841	11 000	0.934
90°	1.560	14 000	0.896

constants at high Reynolds number ($Re > 2 \times 10^4$). An empirical equation was used to relate the loss factor k_i and Reynolds number Re:

$$k_i = \frac{k_o}{1 - \exp(-\frac{Re}{Re_o})} \quad (14)$$

By using the least-square regression, the values of model coefficients k_o, Re_o and coefficient of determination R^2 for door angle $\theta = 30°, 60°, 90°$ were calculated and listed in Table 1. At high Reynolds number, the loss factor k_o increased as the door angle (the effective opening area) decreased. The values of k_o for door angle $\theta = 90°$ (fully open) were very close to the values of k without the door (empty symbol), and the flow resistance ζ_i increased as the door angle decreased.

3.2. Ventilation rate

This section discusses the ventilation rates of wind-driven cross ventilation through a partitioned building. The windward and leeward wall each have one opening at the center, the internal opening is at the corner of the partition wall. Both external and internal openings were square-shaped of different sizes ($d = 40–100$ mm). The fan, porous plate, and nozzle meter were not used in this part of the experiment. The external wind speed $U = 17.5$ m/s, wind direction $\phi = 0°$ for all the cases.

In order to predict the flow rate Q, the measured external pressure coefficients $C_{p1} = 1.0$, $C_{p2} = -0.15$, and the loss factors $k_1 = k_2 = 2.37$ ($C_{d1} = C_{d2} = 0.65$) were used. The internal loss factor k_i was predicted by Eq. (13). The cross-sectional distribution of stream-wise velocity at the internal opening was measured and it was found that the average velocity was very close to the centerline velocity. Therefore, the velocity measured at the centerline was used to represent the average velocity.

Fig. 11 shows the comparison of measured and predicted internal velocities u_i/U. The symbols are the measured velocity, and the solid line is the prediction of Eq. (9). As can seen, the internal

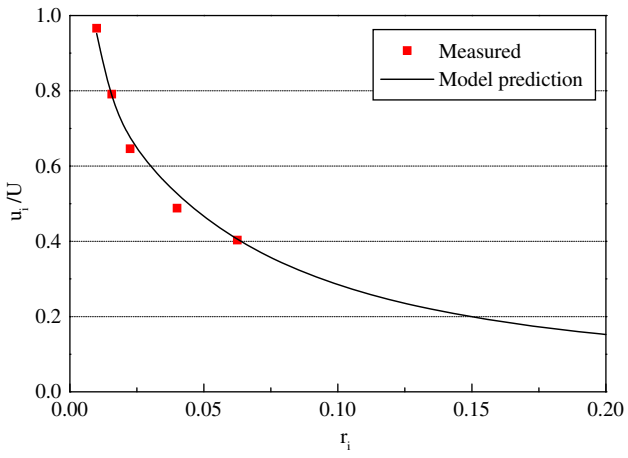

Fig. 11. Dimensionless velocity at the internal opening as a function of internal porosity. Opening ratio $A_2/A_1 = 1$, external porosity $r_1 = 6.25\%$, wind direction $f = 0°$. The solid line is the prediction of Eq. (9).

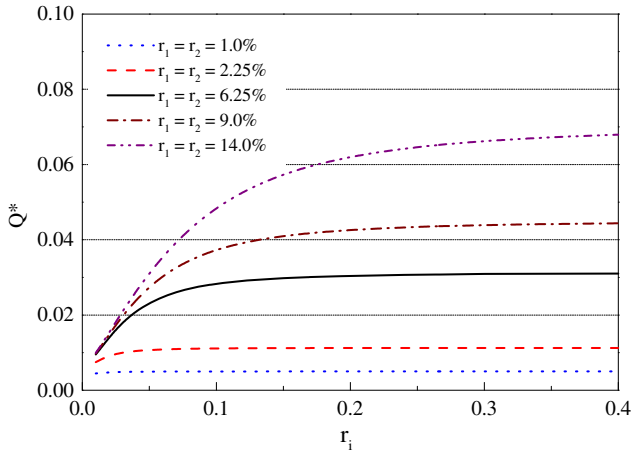

Fig. 12. Dimensionless ventilation rate Q^* as a function of internal porosity. Opening ratio $A_2/A_1 = 1$, wind direction $f = 0°$. The lines are the predicted Q^* by Eq. (7).

velocity u_i/U decreased as the internal porosity r_i increased. The good agreement between the measured and predicted velocities demonstrated that the resistance model can accurately predict the flow rate of partitioned buildings. In addition, the adequacy of the experimental setup and procedure to determine the internal loss factor is justified.

A dimensionless ventilation rate Q^* is defined as:

$$Q^* = \frac{Q}{U \cdot A_w} \tag{15}$$

where A_w is the area of the windward façade. Fig. 12 shows the effect of internal porosity r_i on the ventilation rate Q^* of opening ratio $A_2/A_1 = 1$, wind direction $\phi = 0°$. The lines are the predicted Q^* by Eq. (7) for external porosity $r_1 = r_2 = 1.0\%$, 2.25%, 6.25%, 9%, 14%. As can be seen, the influence of internal porosity r_i on the ventilation rate Q^* is dependent on the external porosity. When the external porosity r_1 and r_2 are less than 3%, the internal porosity r_i has no effect on the ventilation rate Q^*. However, when both r_1 and $r_2 > 5\%$, the values of Q^* increased as the internal porosity r_i increased. This is because the flow resistance of the external opening dominated the ventilation rate when the opening area A_1, A_2 are very small (r_1, $r_2 < 3\%$). But the internal opening A_i (internal resistance) became the dominant parameter when the opening area A_1, A_2 are large (r_1, $r_2 > 5\%$).

4. Conclusions

This study proposed a resistance model to calculate the ventilation rate of wind-driven cross ventilation in partitioned buildings. The flow resistance and loss factors of external and internal openings of various sizes were measured by a high-accuracy fan technique. The relationship between the internal loss factor and discharge coefficient was derived from the energy equation. The experimental results demonstrated that the loss factor of internal opening is dependent on the internal porosity (opening size) and door angle, but is independent of Reynolds number. The loss factor increased as the internal porosity increased and reach a constant value $k = 2.58$ for large opening (porosity ratio $r_i > 5\%$). But the loss factor of a partially open door increased as the door angle (the effective opening area) decreased. In addition, the influence of thickness ratio on the loss factor is much smaller than the internal porosity.

The ventilation rates calculated by the resistance model show good agreement compared with the measured velocities at the internal opening. This implies the resistance model can be used to predict the flow rate of wind-driven ventilation in partitioned buildings. The resistance model indicated that the resistance of the internal opening dominated the ventilation rate when the external openings are large, while the resistances of external openings became the governing parameters when the external porosity is less than 3%.

References

[1] Allard F. Natural ventilation in buildings: a design handbook. London, England: James and James Ltd.; 1998. p. 1–8.
[2] Mochida A, Yoshino H, Takeda T, Kakegawa T, Miyauchi S. Methods for controlling airflow in and around a building under cross ventilation to improve indoor thermal comfort. Journal of Wind Engineering and Industrial Aerodynamics 2005;93:437–49.
[3] Linden PF. The fluid mechanics of natural ventilation. Annual Review of Fluid Mechanics 1999;31:201–38.
[4] Etheridge D, Sandberg M. Building ventilation: theory and measurement. John Wiley and Sons; 1996. p. 93.
[5] Awbi HB. Ventilation of buildings. 2nd ed. Taylor and Francis; 2003. p. 61–62.
[6] Dick JB. The fundamentals of natural ventilation of houses. Journal of the Institution of Heating and Ventilating Engineers 1950;18:179.
[7] ASHRAE. Handbook of fundamentals. American Society of Heating, Refrigerating and Air Conditioning Engineers (ASHRAE); 2009.
[8] Dascalaki E, Santamouris M, Bruant M, Balaras CA, Bossaer A, Ducarme D, et al. Modeling large openings with COMIS. Energy and Buildings 1999;30:105–15.
[9] Miller RW. Flow measurement engineering handbook. 3rd ed. McGraw Hill Co.; 1996. p. 9.8–9.18.
[10] Aynsley RM, Melbourn W, Vickery BJ. Architectural aerodynamics. Applied Science Publishers; 1997. p. 192–194.
[11] Chen Q. Ventilation performance prediction for buildings: a method overview and recent applications. Building and Environment 2009;44:848–58.
[12] Karava P, Stathopoulos T, Athienitis AK. Wind driven flow through openings – a review of discharge coefficients. International Journal of Ventilation 2004;3(3):255–66.
[13] Heiselberg P, Svidt K, Nielsen PV. Characteristics of airflow from open windows. Building and Environment 2001;36:859–69.
[14] Santamouris M, Wouters P. Building ventilation: the state of the art. Earthscan; 2006. p. 41–42.
[15] Heiselberg P, Sandberg M. Evaluation of discharge coefficients for window openings in wind driven natural ventilation. International Journal of Ventilation 2006;5(1):43–52.
[16] Santamouris M. Prediction methods. In: Allard F, editor. Natural ventilation in buildings: a design handbook. James and James Ltd; 1998. p. 100–1.
[17] Tan G, Glicksman LR. Application of integrating multi-zone model with CFD simulation to natural ventilation prediction. Energy and Buildings 2005;37:1049–57.
[18] Chu CR, Chiu YH, Chen YJ, Wang YW, Chou CP. Turbulence effects on the discharge coefficient and mean flow rate of wind-driven cross ventilation. Building and Environment 2009;44:2064–72.
[19] Kurabuchi T, Ohba M, Endo T, Akamine Y, Nakayama F. Local dynamic similarity model of cross-ventilation, Part 1: Theoretical framework. International Journal of Ventilation 2004;2(4):371–82.
[20] Ohba M, Kurabuchi T, Endo Y, Akamine M, Kamata A, Kurahashi T. Local dynamic similarity model of cross-ventilation, Part 2: application of local dynamic model. International Journal of Ventilation 2004;2(4):383–93.
[21] Aynsley R. A resistance approach to analysis of natural ventilation airflow networks. Journal of Wind Engineering and Industrial Aerodynamics 1997;67–68:711–9.
[22] Axley JW, Chung DH. Well-posed models of porous buildings for macroscopic ventilation analysis. International Journal of Ventilation 2006;5(1):89–104.
[23] Idelchik IE. Handbook of hydraulic resistance. 3rd ed. , Boca Raton: CRC Press; 1994. 790 pp.
[24] Chiu YH, Etheridge DW. External flow effects on the discharge coefficients of two types of ventilation opening. Journal of Wind Engineering and Industrial Aerodynamics 2007;95:225–52.
[25] ANSI/AMCA 210-99. Laboratory methods of testing fans for rating. Arlington Height, IL, USA: Air Movement and Control Association International, Inc.; 1999.
[26] Chu CR, Chiu YH, Wang YW. An experimental study of wind-driven cross ventilation in partitioned buildings. Energy and Buildings 2010;42:667–73.

Notation

A_2/A_1: ratio of opening areas (dimensionless)
A_w: cross-section area of wall (m^2)
C_d: discharge coefficient of internal opening (dimensionless)

$C_p = (P - P_o)/0.5\rho U^2$: pressure coefficient (dimensionless)
d: characteristic diameter of opening (m)
k: loss factor of opening (dimensionless)
P_c: pressure at the contraction (internal opening) (Pa)
P_o: reference pressure (Pa)
P_r: room pressure (Pa)
Q^*: dimensionless ventilation rate
$r_i = A_i/A_w$: internal wall porosity (dimensionless)
$t^* = t/d$: thickness ratio of opening (dimensionless)
$Re = u_i d_i/v$: internal opening Reynolds number (dimensionless)
U: external wind speed (m/s)
$u_i = Q_i/A_i$: average velocity at the internal opening (m/s)
z: elevation (m)
ρ: air density (kg/m^3)
ϕ: wind direction (degree)
θ: door angle (degree)
v: kinematic viscosity of air (m^2/s)
ζ: resistance (m^{-4})

Subscripts

1: wind-ward side
2: lee-ward side
e: external
i: internal